Published in final edited form as:
Nat Med. 2008 October ; 14(10): 1112–1117. doi:10.1038/nm.1866.

The CREB Coactivator TORC1 is Required for Energy Balance and Fertility

Judith Y. Altarejos[1], **Naomi Goebel**[1], **Michael D. Conkright**[3], **Hiroshi Inoue**[1], **Xianjin Xie**[4], **Carlos M. Arias**[2], **Paul E. Sawchenko**[2], and **Marc Montminy**[1]

1 *Peptide Biology Laboratories, The Salk Institute for Biological Studies, 10010 N. Torrey Pines Rd. La Jolla, CA. 92037*

2 *Laboratory of Neuronal Structure and Function, The Salk Institute for Biological Studies, 10010 N. Torrey Pines Rd. La Jolla, CA. 92037*

3 *The Scripps Research Institute, 5353 Parkside Drive, Jupiter, FL 33458*

4 *Cell Signaling Technology, 3 Trask Lane, Danvers, MA. 01923*

Abstract

Obesity is a major risk factor in the development of insulin resistance and Type 2 diabetes. Under lean conditions, the adipocyte-derived hormone leptin maintains energy balance by acting on hypothalamic leptin receptors (LRbs) that trigger activation of the JAK2/STAT3 pathway [1–4]. Although disruption of LRb-STAT3 signaling promotes obesity in mice, other neuroendocrine features of LRb function such as fertility appear normal, pointing to a requirement for additional regulators in this setting. Here we show that the cAMP and calcium-responsive CREB coactivator TORC1 is required for energy balance and reproduction; TORC1 −/− mice are hyperphagic, obese, and infertile. Indeed, TORC1−/− females are anovulatory, and they have abnormal uterine morphology along with low circulating concentrations of pituitary luteinizing hormone. Hypothalamic TORC1 was highly phosphorylated and inactive in leptin deficient *ob/ob* mice; and administration of leptin increased amounts of dephosphorylated, nuclear TORC1. Dephosphorylated, active TORC1, in turn, stimulated the expression of CART and KISS1 genes, which encode hypothalamic neuropeptides that mediate leptin effects on satiety and fertility, respectively [5–7]. TORC1 over-expression in cultured hypothalamic cells increased CART and KISS1 gene expression, while depletion of TORC1, by RNAi mediated knockdown in vitro or by targeted gene disruption in vivo, decreased it. Leptin potentiated effects of cAMP and calcium activators on TORC1 transcriptional activity over the CART and KISS1 promoters in cells over-expressing LRb; these effects were disrupted by expression of the dominant negative CREB polypeptide A-CREB. As leptin administration also increased recruitment of hypothalamic TORC1 to CART and KISS1 promoters in vivo, our results indicate that the CREB:TORC1 pathway mediates central effects of hormone and nutrient signals on energy balance and fertility.

Sequestered in the cytoplasm through phosphorylation dependent interactions with 14-3-3 proteins, TORCs (TORC1, TORC2, TORC3) shuttle to the nucleus following their dephosphorylation in response to cAMP and calcium signals, where they potentiate cellular gene expression by binding to CREB over relevant genes [8–12]. TORC1 contains conserved phosphorylation (Ser151) and ubiquitination (Lys575) sites that have been shown to modulate nuclear shuttling and protein stability in TORC2 [13–15] (fig. 1a). By contrast with the

Correspondence: Marc Montminy, Peptide Biology Laboratory, The Salk Institute, 10010 N. Torrey Pines Rd. La Jolla, CA 92037, montminy@salk.edu.

ubiquitous pattern of TORC2 expression, however, TORC1 mRNA and protein are detected in the brain but not in other peripheral tissues such as liver, muscle, or adipose [16] (fig. 1a, sup. fig. 1).

Under basal conditions, TORC1 is highly phosphorylated in cultured hypothalamic GT1-7 cells (fig. 1b) [17]. Exposure to cAMP or calcium activator triggers TORC1 dephosphorylation and nuclear translocation; phosphorylation-defective S151A mutant TORC1 is constitutively nuclear (sup. fig. 1). Over-expression of wild-type TORC1 potentiates CRE-luciferase reporter activity in cells exposed to the cAMP activator forskolin (FSK) or calcium ionophore (A23187); co-treatment with FSK and A23187 increases reporter activity synergistically (fig. 1b). In line with its constitutive nuclear localization, phosphorylation-defective S151A TORC1 strongly upregulates CRE-luciferase activity even under basal conditions. The effects of TORC1 appear CREB dependent because co-expression of a dominant negative CREB polypeptide, called A-CREB [18], disrupts reporter activity in cells exposed to FSK or A23187.

We evaluated the biological role of TORC1 in maintaining energy balance by insertional mutagenesis of the *TORC1* gene with a promoter-less β-galactosidase (β-Geo) gene cassette (fig. 1c). Relative to control littermates, *TORC1* mRNA and protein were undetectable in *TORC1* −/− mice. Consistent with its regulation by the *TORC1* promoter, CNS expression of the β-Geo cassette in *TORC1* mutants mirrored that of endogenous TORC1 protein (fig. 1d, sup. fig. 2). In addition to other brain regions, TORC1 expression was prominent in arcuate and ventromedial nuclei of the hypothalamus. Arguing against significant effects of TORC1 on brain development, however, Nissl-stained sections from *TORC1* −/− brains appear comparable to wild-type (not shown).

TORC1 −/− mice were born at the expected Mendelian frequency, and they were indistinguishable from wild-type controls prior to weaning. Although their linear growth was unimpaired, adult *TORC1* −/− mice were infertile; no offspring were obtained from either *TORC1* −/− males or *TORC1* −/− females mated with wild-type mice (0/6). Anatomically, *TORC1* −/− female uteri appeared threadlike in appearance with noticeable thinning of the endometrium (fig. 1e). Although they had comparable numbers of mature follicles, *TORC1* −/− ovaries contained no corpora lutea, markers of ovulation. Indeed, circulating concentrations of pituitary luteinizing hormone (LH), a key regulator of ovulation, were down-regulated in *TORC1* mutants compared to controls (fig. 1e).

In parallel with these reproductive defects, male and female *TORC1* −/−mice also developed persistent obesity beginning at 9 weeks of age on a normal chow diet (fig. 1f); *TORC1* +/− heterozygotes had intermediate weights relative to wild-type and *TORC1* −/− homozygotes. White adipose mass was increased 2–3 fold in *TORC1* mutant mice, whereas other tissues were relatively unaffected (fig. 1f: sup. fig. 3). Taken together, these results indicate that the effects of TORC1 on body weight are specific to white adipose, affect both males and females, and vary with gene dosage.

We performed metabolic studies to determine why *TORC1* mutant mice gain more weight. Compared with wild-type littermates, *TORC1* −/− animals ate more and they expended less energy at 12 to 14 weeks of age, as determined by physical activity and oxygen consumption monitoring (fig. 2a). Consistent with this disruption, *TORC1* −/− mice were hyperglycemic and hypertryglyceridemic at 9 months of age (fig. 2b). Pointing to the development of insulin resistance, circulating levels of insulin were increased in *TORC1* +/− mice and to a greater extent in *TORC1* −/− homozygotes; they were glucose intolerant by IP glucose-tolerance testing (fig. 2b, c). In line with their obesity, circulating leptin concentrations were also upregulated in *TORC1* −/− mice (fig. 2b).

During feeding, increases in circulating concentrations of leptin as well as insulin and glucose promote satiety and fertility, in part through the activation of arcuate neurons in the hypothalamus [4,19–21]. Realizing that *TORC1* −/− mice are hyperphagic, obese, and infertile, we wondered whether TORC1 is required for the activation of relevant hypothalamic programs in response to feeding signals. Although chronic leptin infusion substantially reduced food intake and body weight in control animals, it had minimal effects on *TORC1*−/− mice (fig. 2d) [22]. Arguing against potential effects on leptin bioavailability, chronic leptin infusion promoted STAT3 phosphorylation a comparable extent in arcuate neurons of wild-type and *TORC1* −/− animals (fig. 2e).

Consistent with the ability for leptin to increase hypothalamic STAT3 activity, mRNA amounts for proopiomelanocortin (*POMC*), neuropeptide Y (*NPY*), and Agouti Related Peptide (*AgRP*), regulatory targets of the LRb-STAT3 pathway that encode anorexigenic (*POMC*) and orexigenic (*NPY, AgRP*) neuropeptides, were comparable between *TORC1* mutants and controls (sup. fig. 4). Indeed, signaling through the downstream melanocortin pathway also appear normal in *TORC1* mutants, because intra-peritoneal (IP) administration of the alpha melanocyte stimulating hormone (α-MSH) analog MTII [23] inhibited food intake to the same extent in both wild-type and *TORC1* −/− mice (sup fig. 5).

We used leptin deficient *ob/ob* mice to determine whether TORC1 activity is disrupted in obesity. Supporting this idea, *ob/ob* mice had increased amounts of phosphorylated, inactive TORC1 in the hypothalamus (fig. 2f). IP leptin injection increased amounts of dephosphorylated, nuclear TORC1 protein in arcuate cells of *ob/ob* mice (fig. 2g). Consistent with a parallel role for nutrient signaling, IP glucose administration also promoted the accumulation of dephosphorylated TORC1 in the hypothalamus (sup fig. 6). Correspondingly, TORC1 was nuclear-localized in arcuate cells during ad libitum feeding but remained cytoplasmic in other regions of the CNS (sup fig. 6). Taken together, these results indicate that hormone and nutrient signals modulate hypothalamic TORC1 activity under lean conditions, and that TORC1 activity is disrupted in obesity.

We performed gene profiling studies to identify hypothalamic genes that contribute to the metabolic and reproductive phenotypes of *TORC1* mutant mice. This analysis revealed that mRNAs for the neuropeptide genes Cocaine and Amphetamine Regulated Transcript (*CART*) and *KISS1* were down-regulated in *TORC1* −/− animals. CART and KISS1 have been found to mediate effects of LRb signaling on feeding and fertility [6,7,24–27]. Indeed, CART is co-expressed with POMC in arcuate neurons, where it inhibits food intake in response to leptin [27], while KISS1 expression in the arcuate promotes reproductive function by stimulating the secretion of hypothalamic gonadotropin releasing hormone (GnRH) [28,29]. Similar to *TORC1* −/− animals, mice with a knockout of *KISS1* have low circulating concentrations of LH, exhibit abnormal uterine morphology, and are infertile [30]. We confirmed that *CART* and *KISS1* genes are down-regulated in *TORC1* −/− mice by Q-PCR and in situ hybridization analysis (fig. 3a,b). As well, hypothalamic staining for kisspeptin, a cleavage product of the KISS1 precursor, was dramatically reduced in arcuate neurons of *TORC1* −/− mice (fig. 3b). Importantly, TORC1 driven β-gal mRNA was co-expressed with CART and KISS1 neuropeptides in arcuate cells by dual immunohistochemistry and *in situ* hybridization (fig. 3c).

Realizing that *CART* and *KISS1* promoters contain CREB binding sites (TGACG/CGTCA) that are conserved between mouse, rat, and human homologs, we considered that TORC1 may regulate both genes via a direct mechanism. Supporting this idea, CREB has been shown to promote *CART* gene expression in response to cAMP [31–33], although a similar role for *KISS1* regulation has not been established. In keeping with its effects on TORC1 dephosphorylation, A23187 treatment increased endogenous mRNA amounts for *CART* and

KISS1 in GT1-7 cells; this induction was blocked in cells depleted of TORC1 by RNAi-mediated knockdown (fig. 3d). Exposure to A23187 or FSK also increased *CART* and *KISS1* reporter activities in transient assays (fig. 4a,b); over-expression of wild-type TORC1, and to a greater extent phosphorylation-defective (S151A) TORC1, enhanced transcription from both promoters. Consistent with the role of CREB in promoting TORC1 recruitment, expression of dominant negative ACREB inhibitor blocked induction of *CART* and *KISS1* reporters by FSK and A23187 (fig. 4a,b).

We performed chromatin immunoprecipitation assays (ChIPs) to determine whether TORC1 and CREB regulate *CART* and *KISS1* genes directly. In line with its constitutive nuclear localization, CREB occupied *CART* and *KISS1* genes in GT1-7 cells comparably under basal conditions and following exposure to FSK or A23187 (fig. 4c). TORC1 occupancy over the *CART* and *KISS1* genes was low under basal conditions - when TORC1 is sequestered in the cytoplasm -and increased following exposure to cAMP or calcium activator - when dephosphorylated TORC1 shuttles to the nucleus and binds to CREB. Consistent with its effect on amounts of nuclear TORC1 protein in the hypothalamus, leptin administration IP also increased TORC1 recruitment to *CART* and *KISS1* promoters in *ob/ob* mice, while CREB occupancy over both genes was constitutive (fig. 4d). Taken together, these results indicate that CREB and TORC1 regulate hypothalamic *CART* and *KISS1* gene expression through a direct mechanism.

Based on their importance for transcriptional induction in response to cAMP and calcium, we wondered whether TORC1 and CREB are also required for effects of leptin on neuropeptide gene expression. Exposure to leptin increased *CART* and *KISS1* reporter activities synergistically with FSK in cells co-transfected with a leptin receptor (LRb) expression vector; these effects were augmented by over-expression of TORC1 (fig. 4e, f). Similar to its effects on cAMP and calcium signaling, ACREB inhibitor blocked induction of both promoters in cells treated with leptin.

Our results indicate that TORC1 is activated by hormonal and nutrient signals in the hypothalamus, where it promotes energy balance and fertility by enhancing CREB activity over relevant neuropeptide genes. Similar to leptin deficent *ob/ob* mice, *TORC1* −/− females have abnormal uterine morphology and low circulating LH levels [34,35]. By contrast with *ob/ob* animals, however, *TORC1* mutant mice are only moderately obese, potentially reflecting compensatory effects of other TORC family members. Consistent with this idea, TORC2 is also expressed in the hypothalamus where it undergoes nuclear shuttling in response to feeding stimuli [36].

In addition to its effects on JAK2/STAT3 signaling, leptin has also been reported to modulate cation channel activity [37,38] and to inhibit the activity of the energy sensing Ser/Thr kinase AMPK [21]. Based on the ability for calcium and AMPK pathways to regulate TORC1 activity, we imagine that these pathways may also mediate effects of leptin on TORC1 in the hypothalamus.

The importance of TORC1 in energy balance appears to be evolutionarily conserved; *Drosophila* TORC, the single fly homolog of mammalian TORCs, is also expressed primarily in the brain where it regulates energy consumption as well as glucose and lipid homeostasis [39]. *Drosophila* TORC and mammalian TORC1 are regulated through phosphorylation by Salt Inducible Kinases (SIKs) and other members of the AMPK family [10,15,39]. Indeed, knockdown of *Drosophila SIK2* in neurons promotes starvation resistance and improves energy balance, suggesting that this Ser/Thr kinase also contributes to effects of hormonal and nutrient signals on hypothalamic TORC1 activity.

Obesity risk in humans has a strong genetic component, which is thought to involve heterozygous loss-of-function mutations in genes that, individually, may display only modest phenotypic changes [40,41]. The presence of hyperphagia, increased adiposity, and insulin resistance even in heterozygous *TORC1* +/− mice suggests that mutations in the *TORC1* gene may also promote the development of obesity in humans. Future epidemiological studies of TORC1 gene mutations in affected populations should provide further insight in this regard.

Methods and Materials

Animals

All animals were housed in a temperature-controlled environment under a 12h light-dark cycle with free access to water and a standard rodent chow diet (Lab Diet 5001), unless otherwise specified. All animal studies were approved by the Salk Institute Institutional Animal Care and Use Committee. *TORC1* mutant mice were generated by insertional mutagenesis. Mouse embryonic stem (ES) cells containing an insertional gene-trap in the *CRTC1* locus (XK522; 129/Ola mouse strain) were obtained from BayGenomics [42,43]. ES cells were injected into C57BL/6 blastocysts to generate chimeric mice, which were backcrossed with C57BL/6 mice (Harlan). Prior to intercrossing, heterozygous mice were backcrossed with C57BL/6 mice for three successive generations. The heterozygous progeny were intercrossed to obtain homozygous, heterozygous and wild-type littermate animals.

Male C57BL/6J, BKS.Cg-*m* +/+ *Leprdb*/J, and B6.V *LepOb* mice were obtained from Jackson Laboratories. All mice were allowed to adapt to their environment for at least 1 week prior to use in studies.

Genotyping

Genomic DNA from tail biopsies was prepared as described previously [44]. Insertion of the pGT0lxf cassette was verified by sequence analysis of PCR-amplified genomic fragments. The following primers were used: A, 5′-GCATCCCTAGCTCTCACTCAGTTAC-3′; and B, 5′-GCGCGTACATCGGGCAAATAA-3′. Genotyping of *TORC1* mutant mice was determined by PCR for the wild-type allele and the mutant allele. The wild-type allele was amplified using primers A and C (5′-ATTCCTCATATACCTCTCTTCTGGTGC-3′). The mutant allele was amplified using primers A and D (5′-GCATGAATCAACTTTGGAGACATGCG-3′).

Measurement of Food Intake and Indirect Calorimetry

Mice were individually housed for at least 3 days prior to the measurement of food intake or calorimetry. Daily food intake of *ad libitum* mice was determined by measuring the weight of food pellets on consecutive days. Locomotor activity, oxygen consumption and carbon dioxide production were simultaneously measured with a Comprehensive Lab Animal Monitoring System (Columbus), as previously described [44]. For nocturnal food intake studies, food was removed from individually housed mice 1h prior to the onset of the dark cycle. Saline, leptin (2μg/g), and MTII (2μg/g) were administered by intraperitoneal injection 30 min prior to the onset of the dark cycle. Food was replaced at the onset of the dark cycle and food intake was measured after 90 min.

Blood and Plasma Measurements

For whole blood and plasma measurements, mouse blood was collected from the tail vein into EDTA-coated capillary tubes (StatSpin). Blood glucose and triglyceride levels were measured with a OneTouch Ultra glucometer (LifeScan) and a CardioChek PA analyzer, respectively. Plasma concentrations of insulin (Mercodia) and leptin (Alpco) were measured by standard immunoassay methods according to the manufacturer's protocol. For serum measurements,

blood was collected by cardiac puncture from anesthetized (350 mg/kg chloral hydrate, i.p.) mice. Serum levels of luteinizing hormone (LH) and follicle-stimulating hormone were determined at the University of Virginia Center for Research in Reproduction Ligand Assay and Analysis Core.

Glucose Tolerance Test

Mice were fasted overnight for 16h and then injected with glucose (2mg/g; i.p.). Blood glucose levels were determined prior to the test and at 15, 30, 60, and 120 min following the injection.

Subcutaneous Infusion

Osmotic minipumps (0.25μL/h, Alzet) were aseptically filled with 0.45 μm-filtered sterile phosphate-buffered saline (PBS) or leptin (1.2mg/mL). Minipumps were primed by incubation at 37°C in sterile 0.9% saline for 8 to 16h. Male 7–8 week old TORC1 −/− mice and wild-type littermates were anesthetized under isoflurane and the minipump was implanted under the dorsal skin between the scapulae. Body weight and food intake were measured daily for 10 days, starting after the implantation of the minipumps. After 10 days of infusion, mice were anesthetized and transcardially perfused for brain immunohistochemistry, as described below.

Intracerebroventricular (ICV) Colchicine Injection

To optimize cellular labeling for CART and KISS1, mice were injected ICV with 5μL of sterile colchicine (2mg/mL), as described previously [45]. Mice were anesthetized with ketamine/xylazine and mounted in a stereotaxic frame. A 33 guage cannula was placed into the lateral cerebral ventricle using the coordinates: +0.3mm anterior-posterior to bregma, +0.8mm lateral to the midline, −2.5mm dorsal-ventral. Colchicine was injected over a 15min period through the cannula using a hamilton syringe. Following injection the cannula was removed and the surgical incision was closed with wound clips. Mice were anesthetized and transcardially perfused for brain immunohistochemistry 36h after colchicine treatment.

Plasmids and Drugs

Expression plasmid for the leptin receptor (LRb) was a gift from Dr. Martin G. Myers Jr. The luciferase reporter plasmid containing sequence from the mouse CART promoter spanning −641 to +30 was kindly provided by Dr. Michael J. Kuhar [31]. The KISS1 luciferase reporter was generated by cloning the human KISS1 promoter spanning −1132 to +1, into pGL2 (Promega). The EVX-1 luciferase reporter and TORC1 expression constructs have been described previously [8]. The S151A TORC1 expression construct was generated by site-directed mutagenesis. Lentiviruses encoding U6 promoter-driven interfering RNAs directed against the TORC1 sequence, 5′-GGTCCCTGCCCAACGTGAAC-3′, were generated as described previously [12]. Forskolin (Sigma), A23187 (Calbiochem), leptin (R and D Systems), and MTII (Bachem) were purchased from the respective manufacturers.

Immunohistochemistry and Immunofluorescence

Mice were anesthetized (350 mg/kg chloral hydrate, i.p.) and transcardially perfused with 4% paraformaldehyde in 0.1M sodium borate buffer at 4°C, as described previously[46]. Brains were post-fixed for 2h at 4°C and then incubated in 0.05 M potassium-PBS (K-PBS) containing 15% (w/v) sucrose 4°C for 12–16 hr. Brains were sectioned on a sliding microtome (25 μM to 30 μM), collected in equally-spaced series and stored in cryoprotectant (20% glycerol and 30% ethylene glycol in 0.1 M phosphate buffer) at −20°C. Immunohistochemistry was conducted on free-floating sections by the avidin-biotin-complex method using the chromogen, diamino-benzidine (Vector Labs). For P-STAT3 (Y705) immunohistochemistry (IHC), sections were pre-treated with 1% H_2O_2 in 1% NaOH for 10 min, 0.3% glycine in K-PBS for 10 min, and 0.03% SDS in K-PBS for 10 min [47]. For TORC1, CART, and KISS1 IHC, sections were pre-

treated with 0.3% H_2O_2 for 10 min and 0.3% glycine, 0.3% Triton X-100 in K-PBS for 10 min. Brain sections were blocked in a K-PBS solution containing 1% Probumin (Millipore), 1% normal donkey serum (Jackson ImmunoResearch) and 0.03% Triton-X-100. Sections were incubated overnight at 4°C with primary antibody diluted in blocking solution. Tissue sections were washed and then incubated with Biotin-SP-conjugated Donkey Anti-Rabbit IgG (1:500, Jackson ImmunoResearch) in blocking solution for 1 hr. Sections were washed and incubated with Vectastain ABC (Vector Labs) for 1 hr. Staining was developed using a Nickel-enhanced diamino-benzidine reaction (Vector Labs). Brain sections were mounted on gelatin-subbed slides, dried, dehydrated and mounted with DPX (Electron Microscopy), unless the sections were also being processed for *in situ* hybridization. In this case, brain sections were mounted on SuperFrost Plus slides (Brain Research Laboratories) and processed for *in situ* hybridization, as described below. The primary antibodies used were P-STAT3 Y705 (1:1000, #9145, Cell Signaling Technologies), KISS1 (1:1000, #9754, Chemicon), CART (1:10000, #6838, PBL-Salk Institute), and TORC1 (1:2500, #6938, PBL-Salk Institute). For TORC1 IHC and IF the antibody was pre-adsorbed against the immunogen carrier β-thryoglobulin and 0.5 mM TORC2 peptide (MESPSTSL), which was synthesized at the Salk Institute Peptide Synthesis Core Facility.

Immunofluorescence was conducted on brain sections or cells fixed with 4% paraformaldehyde in phosphate-buffered saline. Tissue sections or cells were processed as described for immunohistochemistry except the samples were not incubated in hydrogen peroxide and the antigen was visualized using a rhodamine red x-conjugated donkey anti-rabbit antibody (Jackson Immunoresearch).

In Situ Hybridization

Methods for probe synthesis, hybridization and autoradiography as described previously [46]. *In situ* hybridization was conducted using ^{35}S-labelled cRNA probes generated from a rat melanin concentrating hormone (MCH) cDNA [48], a partial β-galactosidase (β-Gal) cDNA (681bp), and full-length mouse CART cDNA. The partial β-Gal cDNA was PCR amplified and cloned from the gene-trap cassette isolated from TORC1 −/− mice. The full-length mouse CART cDNA was cloned from hypothalamic mouse RNA. Brain sections were mounted onto poly-L-lysine coated slides, dried under vacuum, and postfixed with 4% paraformaldehyde for 30 min at 4°C. Tissue sections were digested with proteinase K (10μg/mL) for 30 min at 37° C, acetylated and dehydrated prior to hybridization. Labeled probes ($1–3\times10^9$ dpm/μg) were diluted in hybridization solution, applied to sections and allowed to hybridize overnight at 60° C. Sections were subsequently treated with ribonuclease A (20μg/ml) for 30 min at 37°C, washed with 0.1× SSC buffer (65–85°C), dehydrated and exposed to x-ray films (β-max; Eastman Kodak) for 1–2 d. Slides were then coated with Kodak NTB-2 liquid emulsion, and exposed at 4°C for 3–4 weeks.

Cell Culture, Transfections and Luciferase Assays

The mouse hypothalamic cell line GT1-7 was a gift from Dr. Pam Mellon (UCSD). GT1-7 cells, 293T cells and GH3 cells were cultured in DMEM (Mediatech) containing 10% fetal bovine serum (HyClone), 100 μg/ml penicillin-streptomycin and 1mM pyruvate. Transient transfections of GT1-7 cells were performed using Fugene HD (Roche). HEK293T cells and GH3 cells were transfected by using Lipofectamine 2000 (Invitrogen). For luciferase assays, cells were seeded in 24-well plates and transfected 16h later. Cells were treated for 4h, as indicated, 16 to 48h post-transfection. In reporter assays employing LRb, cells were transfected and treated under serum-free conditions. Cell lysates were prepared and the activities of luciferase and β-galactosidase were determined, as described previously [8].

Brain Region Dissections

Hypothalamic tissue was dissected as described previously [46] with a slight modification. Brains were rapidly removed from anesthetized animals. The brain was sliced coronally with a razor blade to generate a block spanning from the optic chiasm to the rostral end of the mammillary bodies. For RNA isolation or chIP assays the brain slice was immersed in RNA later or ice-cold PBS, respectively. The hypothalamic area was dissected by making two cuts at either end of the optic chiasm and a cut above the third ventricle. These cuts also generated two amygdala-enriched regions, lateral to the hypothalamus, and a cortex-enriched region dorsal to the external capsule. The dissected brain tissue was either snap-frozen for protein extraction or immersed in RNAlater for RNA extractions.

RNA Isolation and Quantitative Real-Time PCR

RNA was isolated from cells using an RNeasy kit (Qiagen) according to the manufacturer's protocol. For tissue, animals were anesthetized (350 μg/kg chloral hydrate, i.p.) and the relevant tissue or brain region was rapidly dissected out and snap-frozen in liquid N_2 or immersed in RNA later for 12 to 16h at 4°C. Total RNA was isolated from the tissue using Trizol reagent (Invitrogen) according to the manufacturer's protocol. Total RNA was then treated with DNase (RNase-Free; Roche) and post-cleaned using an RNeasy kit (Qiagen). 1 μg of total RNA was reverse-transcribed to cDNA using Superscript III (Invitrogen) and random hexamers. cDNAs from samples were amplified and detected using SYBR Green I reagent (Roche) and a LightCycler 480 Instrument (Roche), respectively. Quantification of mRNA levels was performed using the LightCycler 480 Software (Roche) using standard curves and normalizing to β-Actin or L32 expression.

Gene-Profiling Experiments

Male 12-week old wild-type and TORC1 −/− mice (3 of each genotype) were fasted overnight for 15 to 16h and fed a normal chow diet for 6h. Total RNA was isolated from hypothalamic tissue, as described above. Gene-profiling experiments were conducted with an Affymetrix Mouse Genome 430 array and analyzed, as described previously [49].

Chromatin Immunoprecipitation Assays

GT1-7 cells or GH3 cells were plated in 15-cm plates, grown to 80–90% confluency and treated as indicated. For animal experiments, hypothalamic tissue was dissected from mice after the indicated manipulations. Cells or hypothalamic tissue were crosslinked with 1% v/v formaldehyde for 10 min at 4°C, and quenched with 0.125M glycine for 5 min. Chromatin was prepared and immunoprecipitations performed, as described previously [49]. Immunoprecipitations were conducted using antibodies for CREB (#244, PBL-Salk Institute) and TORC1 (#6937E1, PBL-Salk Institute). Rabbit IgG (Santa Cruz) was also utilized as a negative control. Following crosslink reversal, and proteinase K treatment, DNA was isolated by two rounds of phenol-chloroform extractions and ethanol precipitation. DNA was treated with RNase (DNase-free; Roche) and purified with a QIAquick PCR purification kit (Qiagen). Occupancy on target promoters was determined by PCR or quantitative real-time PCR.

Western Blots

Cells or tissue were snap-frozen in liquid N_2 at the end of the experiment. Cells and tissue were lysed in a modified RIPA buffer containing 50 mM Tris pH 7.5 at 4°C, 150 mM NaCl, 1 mM EDTA, 50 mM NaF, 5 mM sodium pyrophosphate, 10 mM β-glycerophosphate, 1% NP-40, 1 mM Na_3VO_4, 0.25% sodium deoxycholate, 0.1% SDS and protease inhibitors (Sigma). The lysate was cleared by centrifugation and the protein concentration of the cleared lysate was determined by the method of Bradford. Western blots for TORC1, TORC2, CREB and P-CREB Ser133 were performed using antibodies 6939E1, 6865, 244, 5322, respectively (Salk

Institute). Antibodies for P-(Ser151) TORC1 and HSP90 were obtained from Cell Signaling and Santa Cruz, respectively.

Cell Counting

P-STAT3 staining and nuclear and cytoplasmic TORC1 staining in hypothalamic sections were quantified by an independent observer in a blinded manner. Five to eight matched arcuate-containing sections from whole-brain series were counted from independent experiments.

Statistical Analyses

Data presented are means ±SEM. Statistical analyses were performed using SigmaStat (Systat). Statistical differences for one factor between two groups or more than two groups were determined using an unpaired Student's *t*-test or an analysis of variance (ANOVA) with a post-hoc test, respectively. Statistical differences for two factors between more than two groups were determined using a two-way ANOVA with a post-hoc test. Values of $P<0.05$ were considered statistically significant.

Supplementary Material

Refer to Web version on PubMed Central for supplementary material.

References

1. Friedman JM. The function of leptin in nutrition, weight, and physiology. Nutr Rev 2002;60:S1–14. [PubMed: 12403078]discussion S68–84, 85–7
2. Bjorbaek C, Kahn BB. Leptin signaling in the central nervous system and the periphery. Recent Prog Horm Res 2004;59:305–31. [PubMed: 14749508]
3. Badman MK, Flier JS. The adipocyte as an active participant in energy balance and metabolism. Gastroenterology 2007;132:2103–15. [PubMed: 17498506]
4. Myers MG, Cowley MA, Munzberg H. Mechanisms of Leptin Action and Leptin Resistance. Annu Rev Physiol 2008;70:537–556. [PubMed: 17937601]
5. Lambert PD, et al. CART peptides in the central control of feeding and interactions with neuropeptide Y. Synapse 1998;29:293–8. [PubMed: 9661247]
6. Kristensen P, et al. Hypothalamic CART is a new anorectic peptide regulated by leptin. Nature 1998;393:72–6. [PubMed: 9590691]
7. Smith JT, Acohido BV, Clifton DK, Steiner RA. KiSS-1 neurones are direct targets for leptin in the ob/ob mouse. J Neuroendocrinol 2006;18:298–303. [PubMed: 16503925]
8. Conkright MD, et al. TORCs: transducers of regulated CREB activity. Mol Cell 2003;12:413–23. [PubMed: 14536081]
9. Iourgenko V, et al. Identification of a family of cAMP response element-binding protein coactivators by genome-scale functional analysis in mammalian cells. Proc Natl Acad Sci U S A 2003;100:12147–52. [PubMed: 14506290]
10. Screaton RA, et al. The CREB coactivator TORC2 functions as a calcium- and cAMP-sensitive coincidence detector. Cell 2004;119:61–74. [PubMed: 15454081]
11. Bittinger MA, et al. Activation of cAMP response element-mediated gene expression by regulated nuclear transport of TORC proteins. Curr Biol 2004;14:2156–61. [PubMed: 15589160]
12. Ravnskjaer K, et al. Cooperative interactions between CBP and TORC2 confer selectivity to CREB target gene expression. Embo J 2007;26:2880–9. [PubMed: 17476304]
13. Dentin R, et al. Insulin modulates gluconeogenesis by inhibition of the coactivator TORC2. Nature 2007;449:366–9. [PubMed: 17805301]
14. Koo SH, et al. The CREB coactivator TORC2 is a key regulator of fasting glucose metabolism. Nature 2005;437:1109–11. [PubMed: 16148943]

15. Katoh Y, et al. Silencing the constitutive active transcription factor CREB by the LKB1-SIK signaling cascade. FEBS J 2006;273:2730–2748. [PubMed: 16817901]
16. Wu Z, et al. Transducer of regulated CREB-binding proteins (TORCs) induce PGC-1alpha transcription and mitochondrial biogenesis in muscle cells. Proc Natl Acad Sci U S A 2006;103:14379–84. [PubMed: 16980408]
17. Liposits Z, et al. Morphological characterization of immortalized hypothalamic neurons synthesizing luteinizing hormone-releasing hormone. Endocrinology 1991;129:1575–83. [PubMed: 1874189]
18. Ahn S, et al. A dominant negative inhibitor of CREB reveals that it is a general mediator stimulus-dependent transcription of c-fos. Molec Cell Biol 1998;18:967–977. [PubMed: 9447994]
19. Bruning JC, et al. Role of brain insulin receptor in control of body weight and reproduction. Science 2000;289:2122–5. [PubMed: 11000114]
20. Parton LE, et al. Glucose sensing by POMC neurons regulates glucose homeostasis and is impaired in obesity. Nature 2007;449:228–32. [PubMed: 17728716]
21. Minokoshi Y, et al. AMP-kinase regulates food intake by responding to hormonal and nutrient signals in the hypothalamus. Nature 2004;428:569–74. [PubMed: 15058305]
22. Halaas JL, et al. Physiological response to long-term peripheral and central leptin infusion in lean and obese mice. Proc Natl Acad Sci U S A 1997;94:8878–83. [PubMed: 9238071]
23. Fan W, Boston BA, Kesterson RA, Hruby VJ, Cone RD. Role of melanocortinergic neurons in feeding and the agouti obesity syndrome. Nature 1997;385:165–8. [PubMed: 8990120]
24. Castellano JM, et al. Expression of hypothalamic KiSS-1 system and rescue of defective gonadotropic responses by kisspeptin in streptozotocin-induced diabetic male rats. Diabetes 2006;55:2602–10. [PubMed: 16936210]
25. Castellano JM, et al. Changes in hypothalamic KiSS-1 system and restoration of pubertal activation of the reproductive axis by kisspeptin in undernutrition. Endocrinology 2005;146:3917–25. [PubMed: 15932928]
26. Popa SM, Clifton DK, Steiner RA. The Role of Kisspeptins and GPR54 in the Neuroendocrine Regulation of Reproduction. Annu Rev Physiol 2008;70:213–238. [PubMed: 17988212]
27. Elias CF, et al. Leptin activates hypothalamic CART neurons projecting to the spinal cord. Neuron 1998;21:1375–85. [PubMed: 9883730]
28. Irwig MS, et al. Kisspeptin activation of gonadotropin releasing hormone neurons and regulation of KiSS-1 mRNA in the male rat. Neuroendocrinology 2004;80:264–72. [PubMed: 15665556]
29. Han SK, et al. Activation of gonadotropin-releasing hormone neurons by kisspeptin as a neuroendocrine switch for the onset of puberty. J Neurosci 2005;25:11349–56. [PubMed: 16339030]
30. d'Anglemont de Tassigny X, et al. Hypogonadotropic hypogonadism in mice lacking a functional Kiss1 gene. Proc Natl Acad Sci U S A 2007;104:10714–9. [PubMed: 17563351]
31. Dominguez G, Lakatos A, Kuhar MJ. Characterization of the cocaine- and amphetamine-regulated transcript (CART) peptide gene promoter and its activation by a cyclic AMP-dependent signaling pathway in GH3 cells. J Neurochem 2002;80:885–93. [PubMed: 11948252]
32. Lakatos A, Dominguez G, Kuhar MJ. CART promoter CRE site binds phosphorylated CREB. Brain Res Mol Brain Res 2002;104:81–5. [PubMed: 12117553]
33. Barrett P, Davidson J, Morgan P. CART gene promoter transcription is regulated by a cyclic adenosine monophosphate response element. Obes Res 2002;10:1291–8. [PubMed: 12490674]
34. Swerdloff RS, Batt RA, Bray GA. Reproductive hormonal function in the genetically obese (ob/ob) mouse. Endocrinology 1976;98:1359–64. [PubMed: 1278106]
35. Barash IA, et al. Leptin is a metabolic signal to the reproductive system. Endocrinology 1996;137:3144–7. [PubMed: 8770941]
36. Lerner RG, Rutter GA, Balthasar N. Hypothalamic CRTC2 activity is regulated by glucose in an AMPK-dependent manner. Nature Medicine. 2008Submitted
37. Cowley MA, et al. Leptin activates anorexigenic POMC neurons through a neural network in the arcuate nucleus. Nature 2001;411:480–4. [PubMed: 11373681]
38. Takahashi KA, Cone RD. Fasting induces a large, leptin-dependent increase in the intrinsic action potential frequency of orexigenic arcuate nucleus neuropeptide Y/Agouti-related protein neurons. Endocrinology 2005;146:1043–7. [PubMed: 15591135]

39. Wang B, et al. The insulin-regulated CREB coactivator TORC promotes stress resistance in Drosophila. Cell Metab 2008;7:434–44. [PubMed: 18460334]
40. Chung WK, et al. Heterozygosity for Lep(ob) or Lep(rdb) affects body composition and leptin homeostasis in adult mice. Am J Physiol 1998;274:R985–90. [PubMed: 9575960]
41. Farooqi S, O'Rahilly S. Genetics of obesity in humans. Endocr Rev 2006;27:710–18. [PubMed: 17122358]
42. Skarnes WC, et al. A public gene trap resource for mouse functional genomics. Nat Genet 2004;36:543–4. [PubMed: 15167922]
43. Stryke D, et al. BayGenomics: a resource of insertional mutations in mouse embryonic stem cells. Nucleic Acids Res 2003;31:278–81. [PubMed: 12520002]
44. Qi L, et al. TRB3 links the E3 ubiquitin ligase COP1 to lipid metabolism. Science 2006;312:1763–6. [PubMed: 16794074]
45. Sawchenko PE, Swanson LW, Vale WW. Corticotropin-releasing factor: co-expression within distinct subsets of oxytocin-, vasopressin-, and neurotensin-immunoreactive neurons in the hypothalamus of the male rat. J Neurosci 1984;4:1118–29. [PubMed: 6609226]
46. Reyes TM, et al. Urocortin II: a member of the corticotropin-releasing factor (CRF) neuropeptide family that is selectively bound by type 2 CRF receptors. Proc Natl Acad Sci U S A 2001;98:2843–8. [PubMed: 11226328]
47. Munzberg H, et al. Appropriate inhibition of orexigenic hypothalamic arcuate nucleus neurons independently of leptin receptor/STAT3 signaling. J Neurosci 2007;27:69–74. [PubMed: 17202473]
48. Bittencourt JC, et al. The melanin-concentrating hormone system of the rat brain: an immuno- and hybridization histochemical characterization. J Comp Neurol 1992;319:218–45. [PubMed: 1522246]
49. Zhang X, et al. Genome-wide analysis of cAMP-response element binding protein occupancy, phosphorylation, and target gene activation in human tissues. Proc Natl Acad Sci U S A 2005;102:4459–64. [PubMed: 15753290]

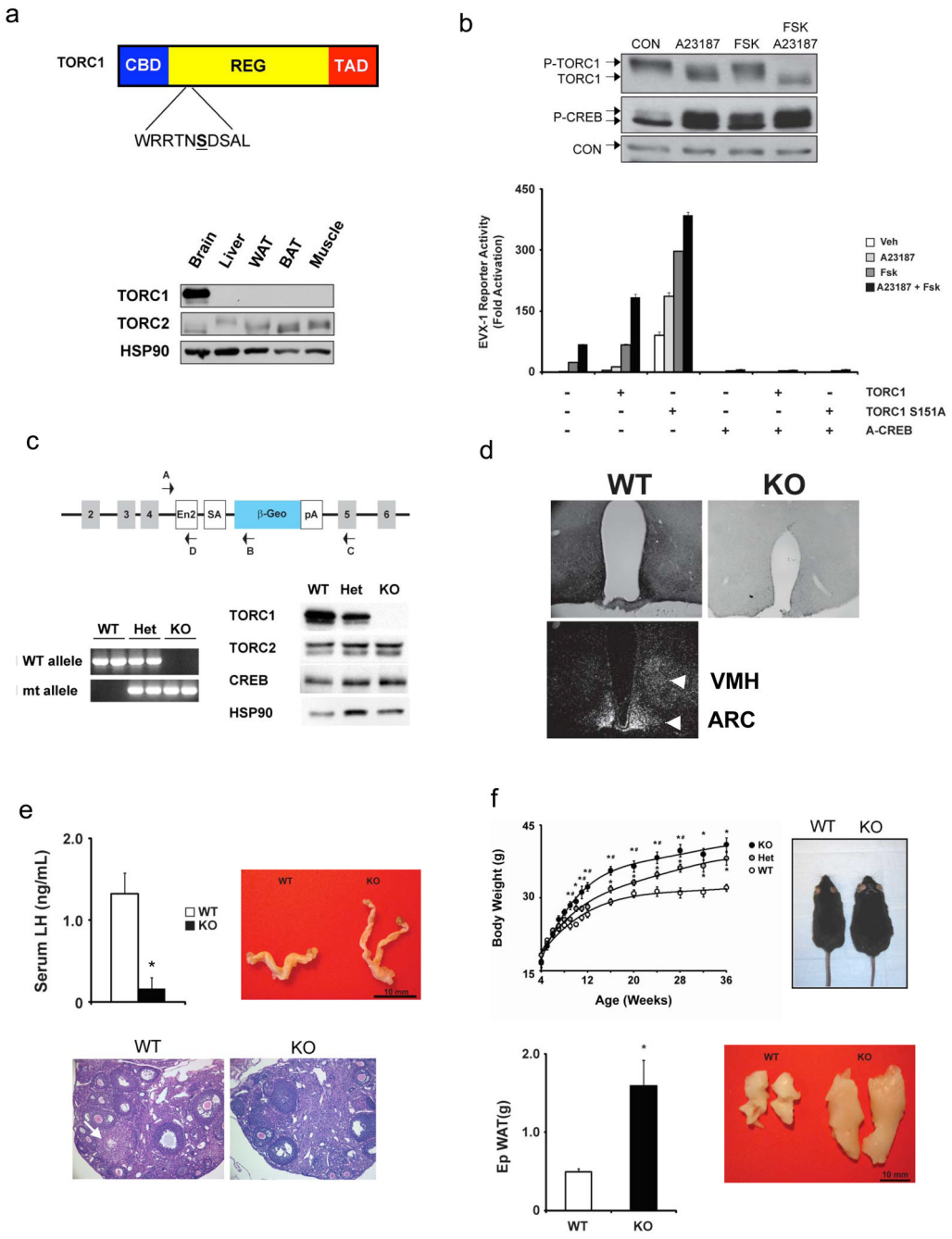

Figure 1.

Mice with a knockout of *TORC1* are obese and infertile. A. Top, schematic of TORC1 showing conserved CREB binding domain (CBD) as well as regulatory (REG) and transcriptional activation (TAD) domains; inset shows sequence of regulatory Ser151 site (bolded), which sequesters TORC1 in the cytoplasm following its phosphorylation by members of the AMPK family of Ser/Thr kinases. Bottom, immunoblot of TORC1 protein amounts in various tissues. B. Top, immunoblot showing effect of calcium ionophore (A23187; 1μM) and FSK (1μM) on amounts of slower-migrating phospho-TORC1 and faster-migrating unphosphorylated TORC1 (P-TORC1 and TORC1, respectively) in hypothalamic GT1-7 cells. Amounts of Ser133-phosphorylated CREB (P-CREB) indicated. Bottom, transient assay showing effect of

wild-type TORC1 or S151A mutant TORC1 on CRE-luc reporter activity in cells exposed to FSK (1μM) and A23187 (1μM); cells expressing dominant negative CREB polypeptide A-CREB indicated. Data are representative of at least three independent experiments. $P<0.05$ for multiple comparisons between the groups is considered statistically significant. Pertinent comparisons are discussed in the text. C. Top, schematic showing disruption of the *TORC1* gene through insertion of the gene trap vector pGT0lxf containing Engrailed 2 (EN2) sequences, splice acceptor (SA), β-galactosidase-neomycin resistance (β-Geo) gene cassette, and polyadenylation sequence (pA) between exons 4 and 5, within the coding region (between aa. 148–149) of the *TORC1* gene. Primers used to verify insertion of the gene trap (A and B) and for genotyping animals (A, C and D) indicated. Bottom left, PCR analysis of genomic DNA from wild-type, *TORC1* +/− (het), and *TORC1* −/− (ko) mice showing presence of wild-type (detected with primers A and C) and mutant (detected with primers A and D) TORC1 alleles. Bottom right, immunoblot showing relative TORC1 protein amounts in whole brain extracts from wild-type, *TORC1* +/−, and *TORC1* −/− mice. Amounts of CREB and TORC2 protein also indicated. D. Immunohistochemical analysis of TORC1 expression in the hypothalamus. Top, TORC1 protein staining in arcuate and ventromedial nuclei in wild-type (left) or *TORC1* −/− mice (right). Bottom, TORC1 promoter activity in hypothalamic sections from *TORC1* −/− mice, evaluated by in situ hybridization analysis using inserted β-galactosidase (β-Geo) probe. E. Top left, plasma levels of luteinizing hormone in *TORC1* −/− and wild-type female littermates (*; $P<0.05$, n=3). Top right, relative uterine morphology in control and TORC1 knockout mice. Bottom, Hematoxylin-Eosin staining of ovarian sections from wild-type and *TORC1* −/− mice. Arrow points to corpus luteum in wild-type but not KO mice. F. Top left, relative weights of wild-type, *TORC1* +/−, and *TORC1* −/− mice from 4 to 36 weeks of age (*; $P<0.05$ compared to wild-type mice; $^{\#}$, $P<0.05$ compared to *TORC* +/− mice, n=6–37; data are means±s.e.m.). Right, appearance of wild-type and *TORC1* −/− littermates at 36 weeks. Bottom, epididymal fat pad mass in 36 week old control and *TORC1* −/− mice. (*; $P<0.05$, n=6–10 per group)

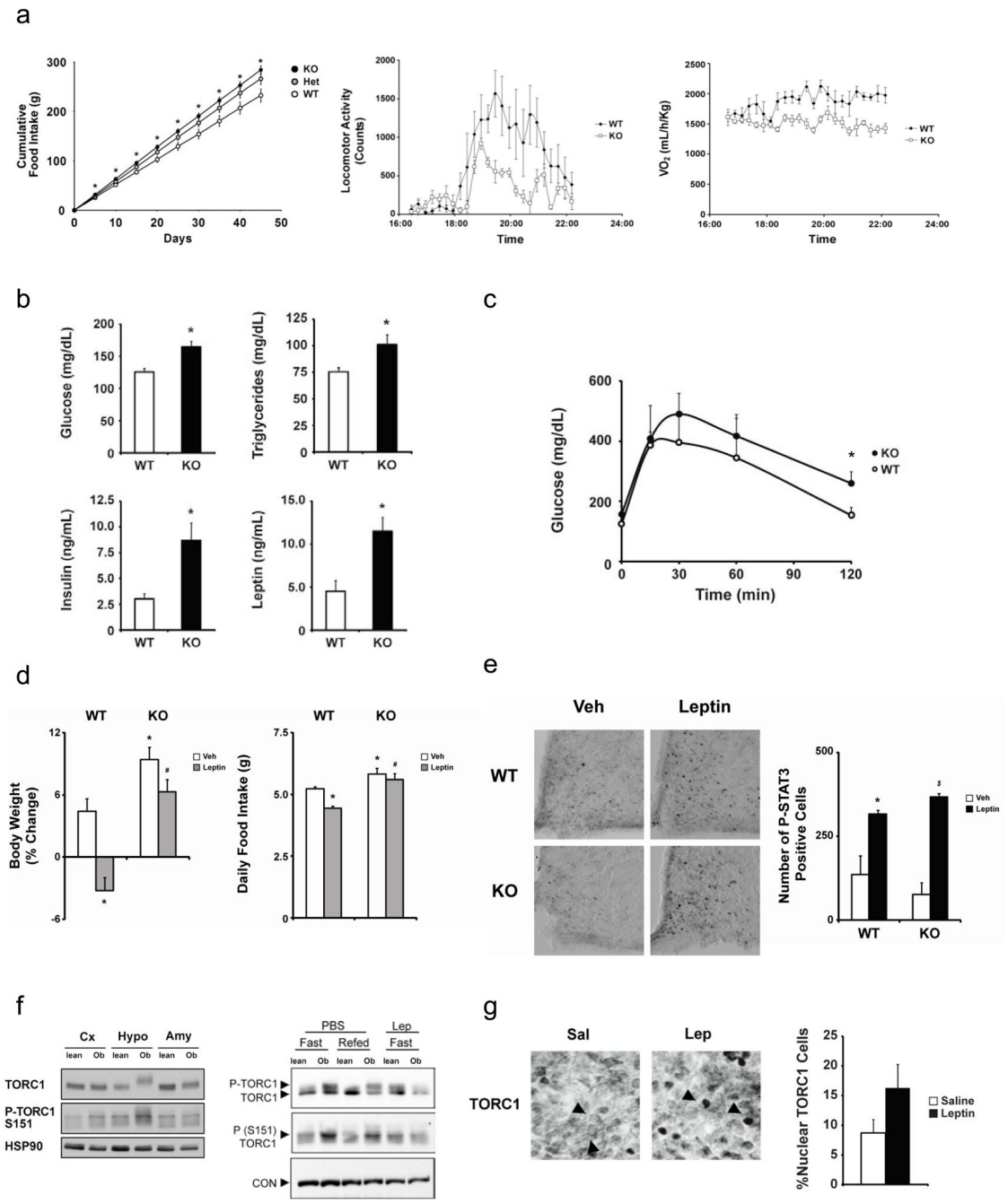

Figure 2.

TORC1 −/− mice are hyperphagic and have reduced energy expenditure. A. Left, cumulative food intake over a 45 day interval, beginning at 12 weeks of age, in *TORC1* −/−, *TORC1* +/−, and wild-type littermates maintained on a normal chow diet (*; $P<0.05$, n=7–8; data are means ±s.e.m.). Physical activity (center) and oxygen consumption (right) in 14 week old *TORC1* −/− and control littermates (n=4 mice per group). B. Circulating glucose (top left), and triglyceride (top right) concentrations in 36 week old wild-type, *TORC1* +/−, and *TORC1* −/− mice (*; $P<0.05$, n=5–8 per group). Bottom, circulating plasma insulin (left) and leptin (right) concentrations (*;$P<0.05$, n=5–12 per group). C. Glucose tolerance testing (*; $P<0.05$, n=4–5) of wild-type and *TORC1* −/− animals. D. Effect of subcutaneous infusion of vehicle or leptin

(10 days; 300ng/h) on body weight (left) and average daily food intake (right) in wild-type and *TORC1* −/− mice (*; $P<0.05$ compared to vehicle-infused wild-type mice; $^{\#}$, $P<0.05$ compared to leptin-infused wild-type mice, n=5–7; data are means±s.e.m.). E. Left, effect of leptin or vehicle infusion (see panel D) on P-STAT3 staining in arcuate cells of wild-type and *TORC* −/− mice. Right, cell counts for P-STAT3-positive cells in vehicle or leptin-infused wild-type and *TORC* −/− mice (*; $P<0.05$ compared to vehicle-infused wild-type mice; $^{\$}$, $P<0.05$ compared to vehicle-infused *TORC* −/−mice, n=3; data are means±s.e.m.). F. Left, immunoblot showing amounts of total and phospho (Ser151)TORC1 in cortex (Cx), hypothalamus (Hypo), and amygdala (Amy) from lean or leptin deficient *ob/ob* mice. Right, immunoblot showing effect of leptin or saline (PBS) injection IP on amounts of total and phospho (Ser151)TORC1 in hypothalamic extracts from lean and *ob/ob* mice under fasted or refeeding conditions. G. Left, immunohistochemical analysis of TORC1 staining in representative arcuate sections from *ob/ob* mice injected (IP) with leptin (3μg/g) or saline control. Arrows point to predominant cytoplasmic TORC1 staining in control sections and nuclear TORC1 staining in leptin-treated sections. Right, graph showing % TORC1-positive nuclei identified in hypothalamic sections from saline or leptin treated *ob/ob* mice.

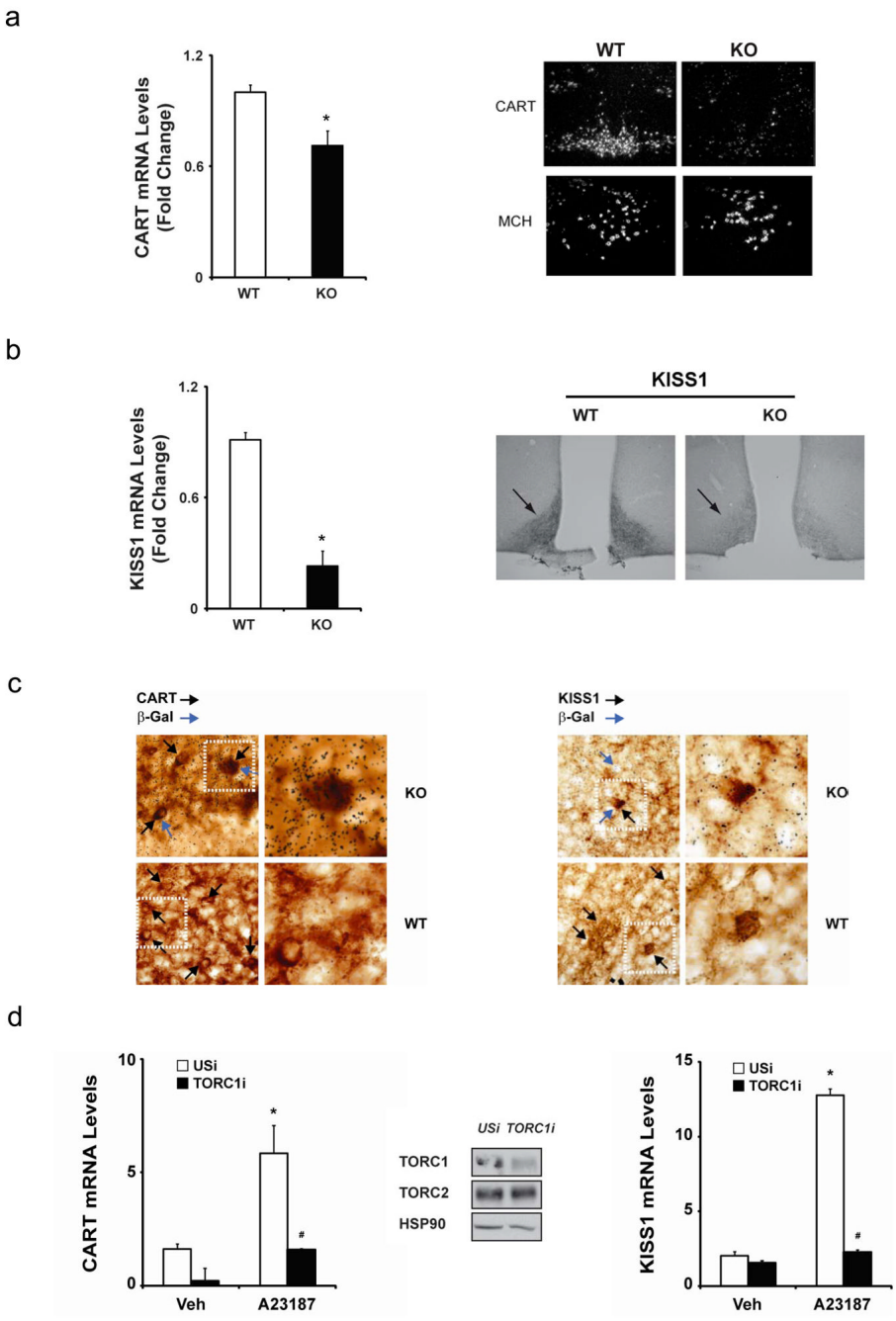

Figure 3.

Reduced hypothalamic expression of anorexigenic and reproductive neuropeptide genes in *TORC1* −/− mice. A. Q-PCR (left) (*; $P<0.05$, n=3) and in situ hybridization (right) analysis of CART mRNA amounts in wild-type and *TORC1* −/− mice. In situ hybridization analysis of melanin concentrating hormone (MCH) mRNA in wild-type and *TORC1* −/− mice shown for comparison. B. Q-PCR (left) (*; $P<0.05$, n=5–6) and immunohistochemical analysis (right) of KISS1 expression in hypothalami of *TORC1* −/− and control littermates. Right, relative kisspeptin staining in arcuate sections from wild-type and TORC1−/− mice using anti-kisspeptin-10 antiserum. C. Left, dual immunohistochemistry and *in situ* hybridization for CART and TORC1 promoter-driven β-Gal, respectively, in colchicine-treated *TORC1* −/−

mice and control littermates. Right, dual immunohistochemistry and *in situ* hybridization for KISS1 and β-Gal, respectively, in colchicine-treated *TORC1* −/− mice and control littermates. Black arrows indicate cells with positive immunostaining. Blue arrows indicate cells positive for β-Gal mRNA. White boxes outline the magnified inset shown to the right of the corresponding panel. D. Effect of A23187 exposure (1μM; 2 hours) on mRNA amounts for *CART* (left) and *KISS1* (right) in control and *TORC1*-depleted GT1-7 cells (*; $P<0.05$ compared to vehicle-treated cells expressing unspecific RNAi; #, $P<0.05$ compared to A23187-treated cells expressing unspecific RNAi, data are means±s.e.m.). Middle, immunoblot showing effect of RNAi-mediated *TORC1* knockdown on TORC1 protein amounts relative to control cells expressing unspecific (USi) RNAi.

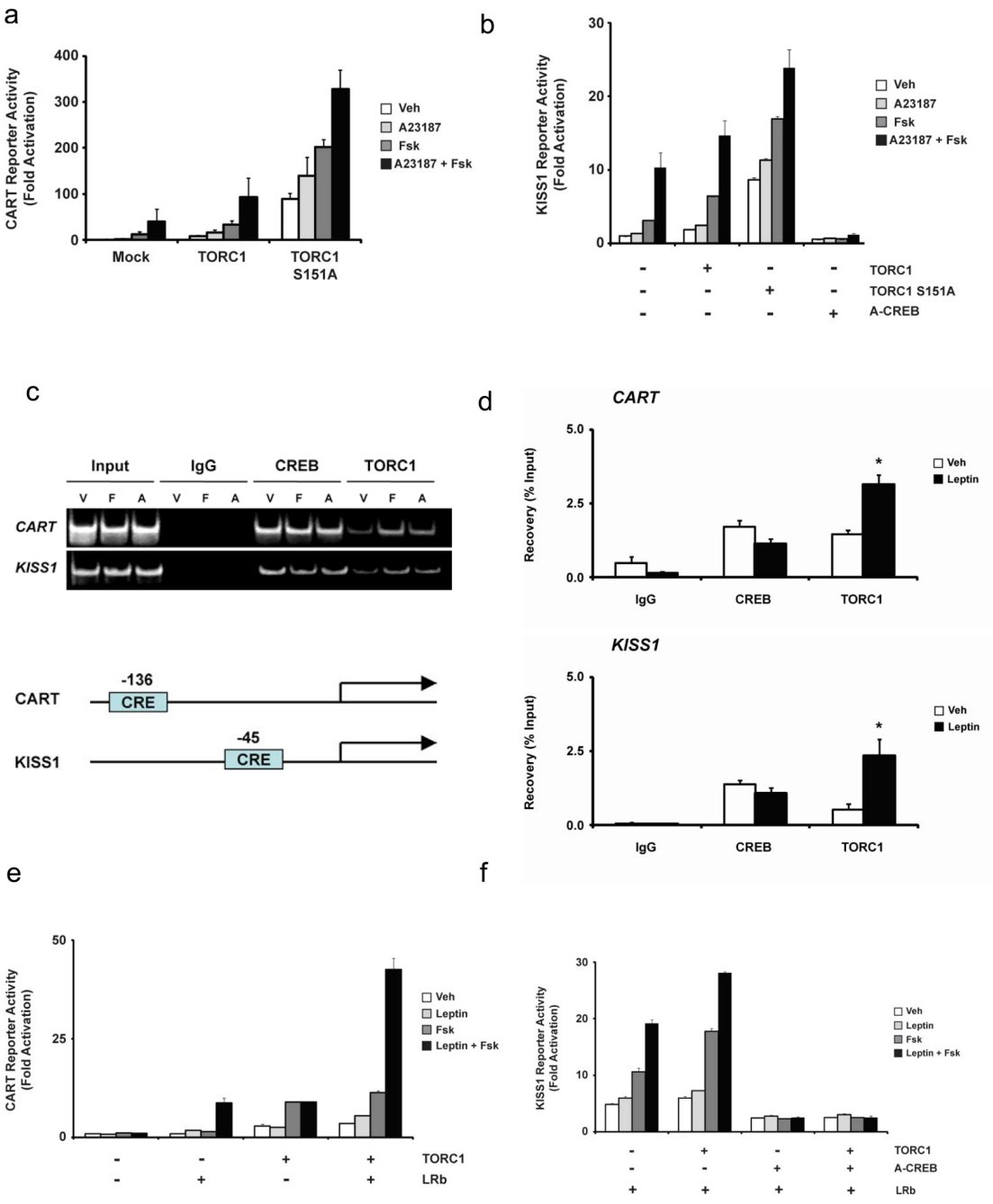

Figure 4.

CART and *KISS1* genes are direct targets of TORC1 and CREB in the hypothalamus. A. and B. Transient transfection assay of HEK293T cells using *CART*-luciferase (A) and *KISS1*-luciferase (B) reporters. Exposure to FSK (1μM) and A23187 (1μM), alone or in combination, indicated. Relative effect of wild-type TORC1 and phosphorylation-defective S151A TORC1 expression on reporter activity shown. Co-transfection of dominant negative A-CREB expression plasmid indicated. Data are representative of at least three independent experiments. $P<0.05$ for multiple comparisons between the groups is considered statistically significant. Pertinent comparisons are discussed in the text. C. Top, chromatin immunoprecipitation (ChIP) assay of GT1-7 cells exposed to FSK (F; 1μM), A23187 (A; 1μM), or vehicle (V) for 1 hour.

Recovery of *CART* and *KISS1* promoter fragments from immunoprecipitates of CREB and TORC1 relative to control IgG shown. Input amounts of *CART* and *KISS1* promoter DNA indicated. Bottom, schematic of *CART* and *KISS1* promoters showing location of conserved CREB binding sites (CRE) relative to the transcription start site. D. ChIP assay of hypothalamic tissue from *ob/ob* mice injected IP with saline (Veh) or leptin (3μg/g) for 1 hour. Relative occupancy of hypothalamic CREB and TORC1 over *CART* and *KISS1* promoters in control and leptin-injected mice indicated. CREB and TORC1 occupancy is statistically significant compared ($P<0.05$) to the relevant IgG controls. * indicates $P<0.05$ compared to hypothalami from vehicle-treated *ob/ob* mice. E. and F. Transient transfection assay of HEK293T cells using *CART* (E) or *KISS1* (F) luciferase reporters. Effect of leptin treatment (100nM) on reporter activity in control and leptin receptor (LRb) expressing cells shown; co-treatment with FSK (1μM) indicated. Expression of wild-type TORC1 or phosphorylation-defective S151A TORC1 indicated. Effect of dominant negative A-CREB on reporter activity shown. $P<0.05$ for multiple comparisons between the groups is considered statistically significant. Pertinent comparisons are discussed in the text.